# Temperature Study of an Experimental Segmental Concrete Bridge

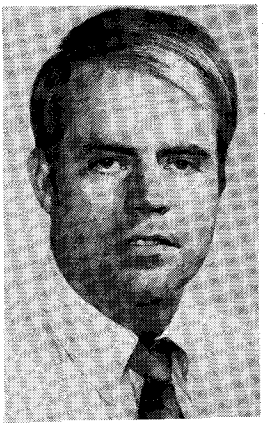

**P. C. Hoffman**
Assistant Professor of Civil Engineering
Villanova University
Villanova, PA

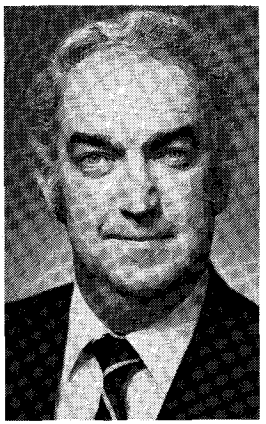

**R. M. McClure**
Associate Professor of Civil Engineering
The Pennsylvania State University
University Park, PA

**H. H. West**
Associate Professor of Civil Engineering
The Pennsylvania State University
University Park, PA

Several bridge distresses have been attributed to temperature variations within the structures.[1,2] Consequently, bridge designers are utilizing various design approaches for the evaluation of temperature variations in bridge members and for the subsequent determination of stresses and strains.

This article presents the findings from field temperature measurements of an experimental segmental bridge. A comparison with some currently accepted design temperature distributions is performed. The current temperature distributions for design were modified to agree with actual measured values in order to allow a direct comparison. Finally, from the numerical comparisons, some disagreements with current approaches are highlighted.

## THE TEMPERATURE PROBLEM

The temperature problem is caused by the thermal environment (see Fig. 1). Surface temperatures of a cross section result from numerous random inputs, namely, the surrounding air temperature, the solar energy striking some surfaces, convection caused by the wind vector, and various forms of precipitation.

Presents the major findings from field temperature measurements of an experimental segmental box girder bridge. Compares the New Zealand and PCI-PTI methods of temperature distribution and by means of numerical examples highlights the differences between the various approaches.

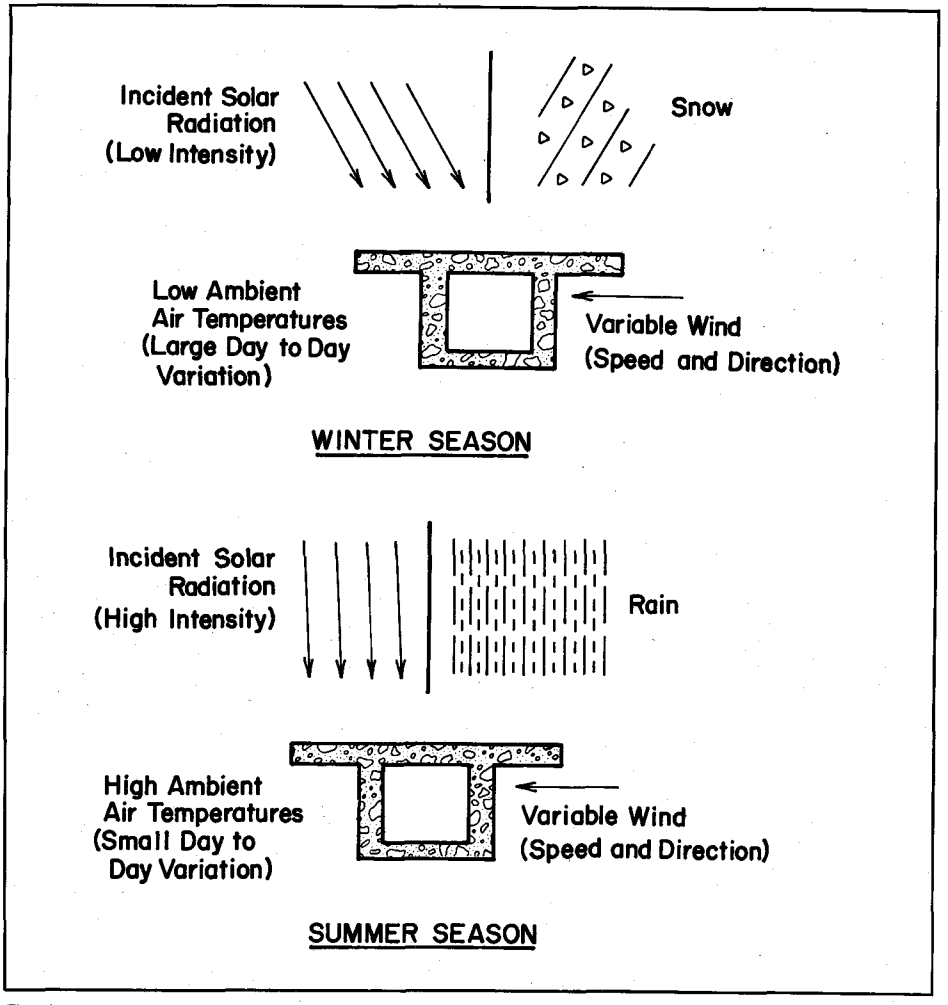


Fig. 1. The thermal environment surrounding a box girder during the winter and summer seasons.

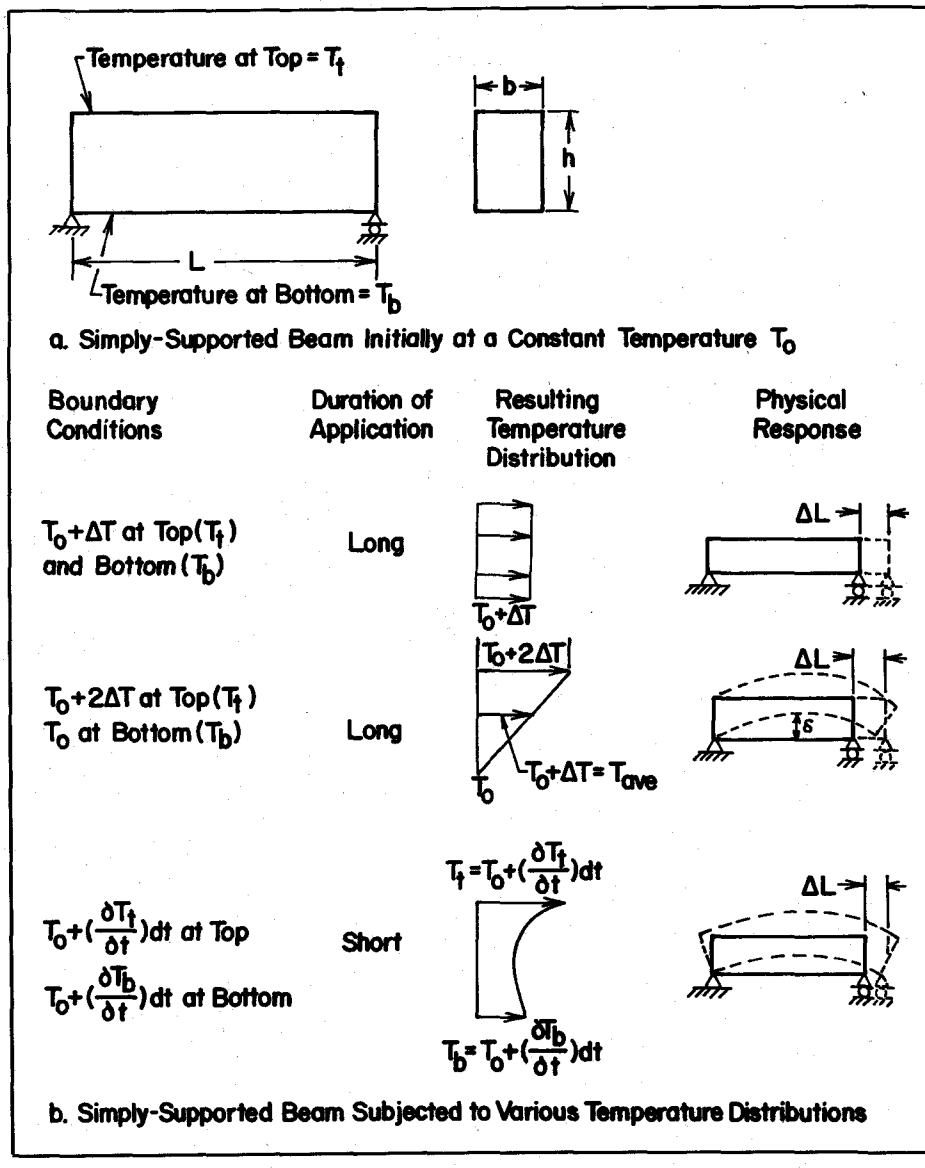


Fig. 2. Influence of thermal boundary conditions on a simply supported beam.

These inputs not only vary from season to season but also throughout any given day (diurnal cycle). Such a random and transient set of thermal parameters leads to an ever-changing set of cross-sectional surface temperatures. Since the boundary conditions are continually changing, the temperature distribution within a cross section must also vary with time.

The significance of a transient heat flow condition can best be described by considering a simply-supported beam initially at a constant temperature ($T_o$) (Fig. 2a). If both the top and bottom surfaces are subjected to a temperature

change ($\Delta T$), then, over some period of time, the cross section will be subjected to a new uniform temperature ($T_o + \Delta T$). The physical response of the beam will then be an elongation ($\Delta L$) which is a stress-free strain (Fig. 2b).

On the other hand, if only the top surface is subjected to an increased temperature ($2\Delta T$), then, over some time period, a linear temperature distribution will occur. Under the linear temperature distribution, the beam will elongate ($\Delta L$) and bow upwards. Again, strain will occur without the development of stress (Fig. 2b).

In actuality, because surface temperatures vary with time, a nonlinear temperature distribution will be present. In other words, before a steady state heat conduction condition can be reached, the boundary conditions will have changed. Since the physical response of the beam requires that plane sections remain plane, there can only be an elongation and curvature (Fig. 2b). Thus, a residual stress must develop, which is given by the formula:

$$f_r(y) = E\,[\phi\, y + \epsilon_{ave} - \alpha t(y)] \qquad (1)$$

where

$f_r(y)$ = residual stress $y$ distance from neutral axis
$E$ = modulus of elasticity
$\phi$ = curvature
$y$ = distance from neutral axis to fiber where residual stress is designated
$\epsilon_{ave}$ = average strain caused by mean temperature change
$\alpha$ = coefficient of thermal expansion
$t(y)$ = temperature change $y$ distance from neutral axis

A more detailed explanation of Eq. (1) is presented in the Appendix.

In order to find the residual stress using Eq. (1), the curvature and average strain due to the temperature distribution must be determined. Using the Bernoulli-Navier principle, and assuming a one-dimensional temperature distribution, Priestley[3,4] used equilibrium conditions to develop the following expression for curvature:

$$\phi = \frac{\alpha}{I} \int t(y) \cdot b(y) \cdot y \cdot dy \qquad (2)$$

where

$I$ = second moment of area about the neutral axis, and
$b(y)$ = width of section $y$ distance from neutral axis

The uniform strain due to the mean temperature differential is readily computed as:

$$\epsilon_{ave} = \frac{\alpha}{A} \int t(y) \cdot b(y) \cdot dy \qquad (3)$$

where $A$ is the cross-sectional area.

Therefore, for a given temperature distribution, curvature and the uniform strain can be computed for Eqs. (2) and (3), respectively, which, in turn, can be used in Eq. (1) to determine the residual stress.

In summary, the response to the nonlinear temperature distribution can be broken into three parts as shown in Fig. 3. The first part consists of the uniform structural distortion due to the uniform seasonal temperature input, which is currently addressed in most design specifications. The second part occurs when the temperature change (distribution), as referenced from the seasonal value, is applied, causing an incremental change to take place in the uniform temperature to form an overall uniform mean temperature. Finally, the third part involves a nonlinear temperature distribution as measured about the overall mean temperature.

Currently, American design codes do not specify the consideration of an incremental uniform temperature change (Part II) nor a nonlinear temperature distribution (Part III). For example, the Standard Specifications for Highway Bridges of the American Association of

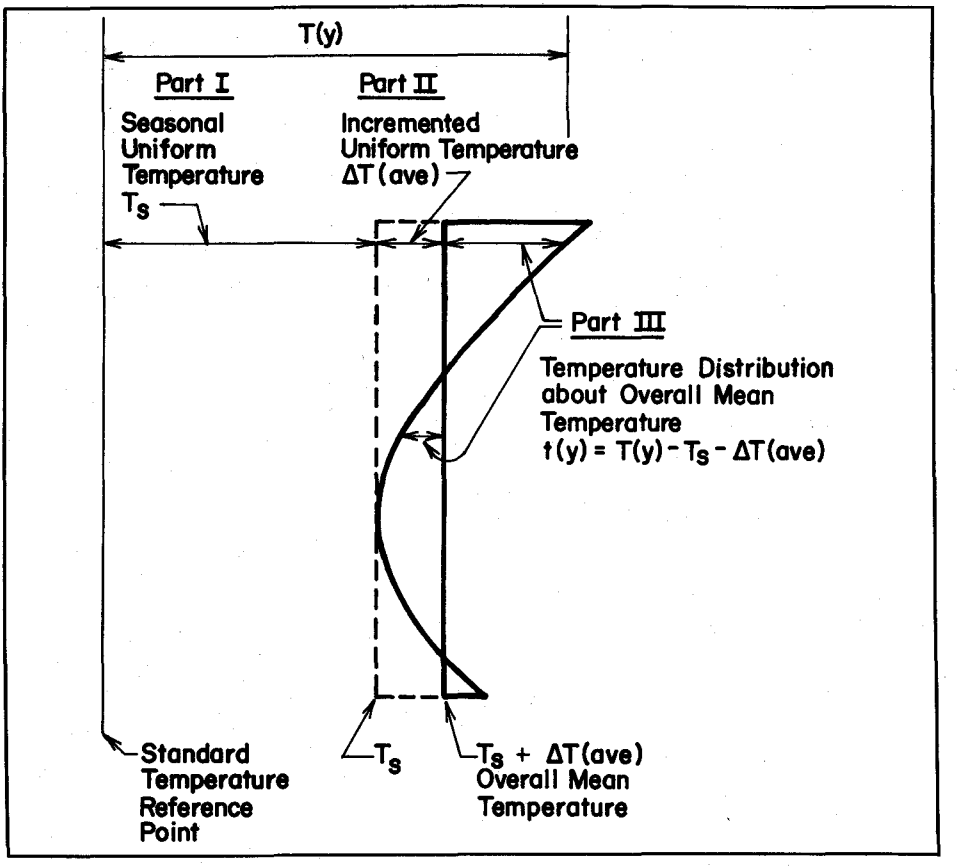


Fig. 3. Three-part input to the thermal distribution problem.

State Highway and Transportation Officials permits stress increases of 25 to 40 percent for load combinations involving temperature and shrinkage effects;[5] however, the actual specification of a critical temperature distribution and the subsequent analysis of curvature and residual stresses are not specified.

Contrary to such American code practices, the New Zealand Specification[4] requires the consideration of a fifth-power temperature distribution, as shown in Fig. 4(a). For the web of a box section and the cantilever flanges, the temperature distribution is taken as 32°C (57.6°F) at the top surface without blacktop, and it decreases with depth according to the fifth power and becomes zero at 1200 mm (47.2 in.). After 1200 mm (47.2 in.), the member is considered too massive to be affected by rapid temperature changes in the diurnal (daily) cycle.

In addition, a linear temperature distribution is assumed in the soffit, which is 1.5°C (2.7°F) at the lower surface and decreases to zero at 200 mm (7.9 in.). The deck slabs above the cells are subjected to a linear temperature distribution of 32°C (57.6°F) on the surface, decreasing 0.05°C per mm (2.3°F per in.).

In the *Precast Segmental Box Girder Bridge Manual*[6] (published jointly by the Prestressed Concrete Institute and the Post-Tensioning Institute), a

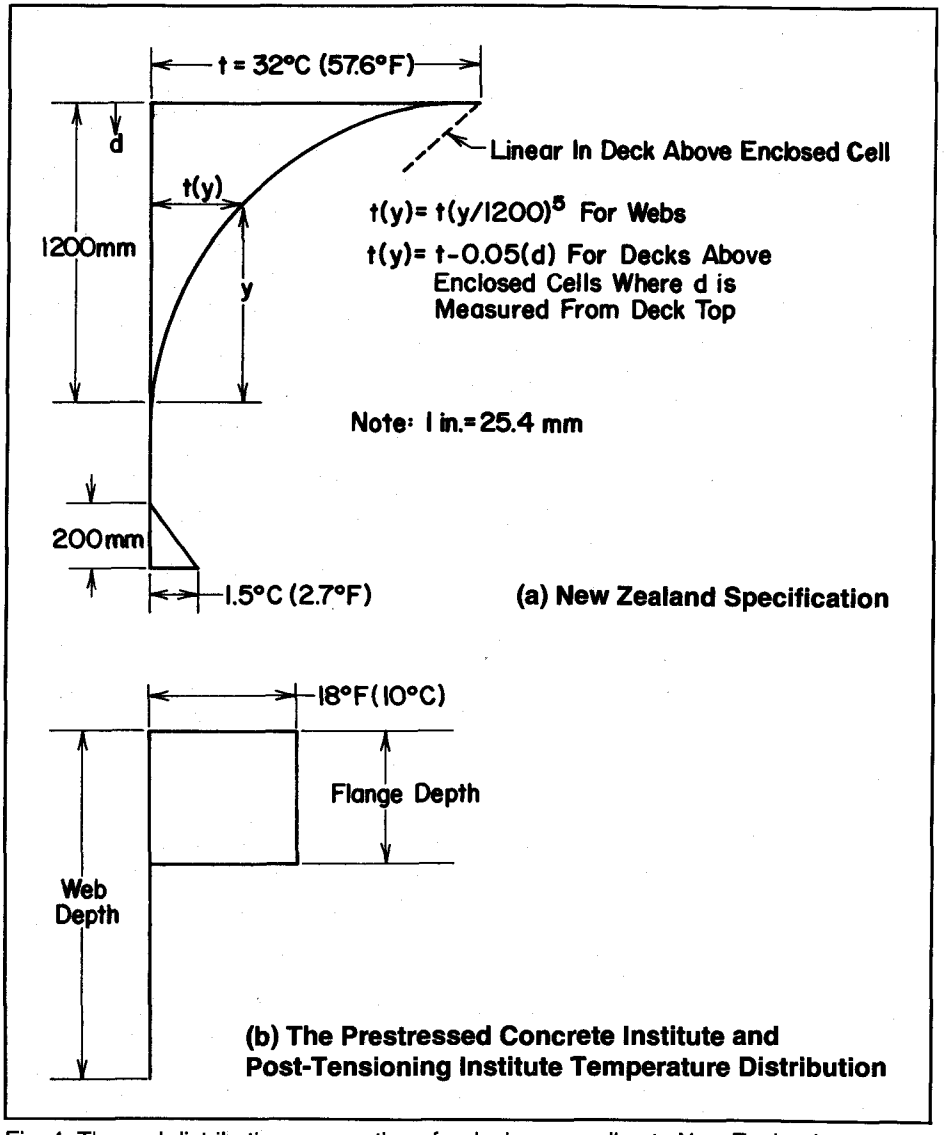


Fig. 4. Thermal distribution assumptions for design according to New Zealand Specification and PCI-PTI method.

method is given which allows for temperature distribution where the flange is 18°F (10°C) warmer than the remaining cross section, as shown in Fig. 4(b). Although the New Zealand approach is much more sophisticated than the PCI-PTI method, a question arises concerning the relative accuracy of the two approaches. Finding the answer to this question was one of the primary objectives of a year-long temperature study on an experimental prestressed segmental box bridge.[7] The findings, with respect to the question of accuracy versus complexity, are presented in the numerical examples that follow.

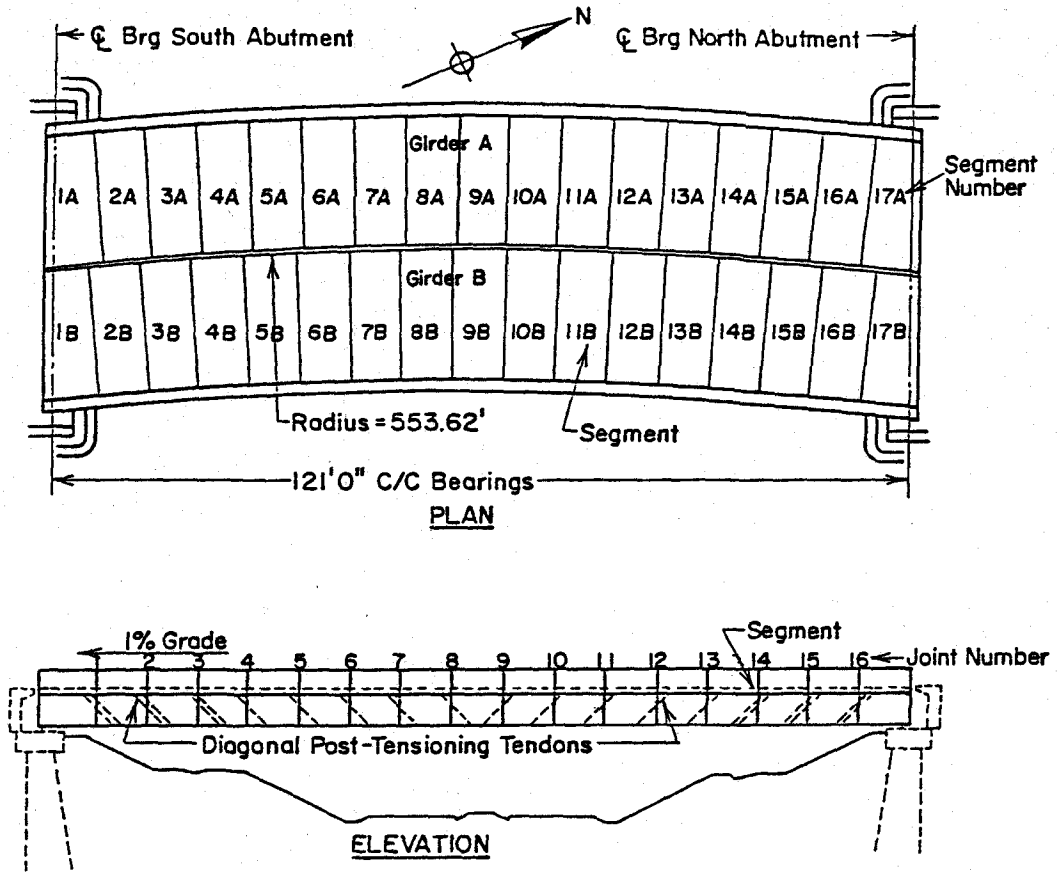


Fig. 5a. General plan and elevation of experimental segmental box girder bridge.

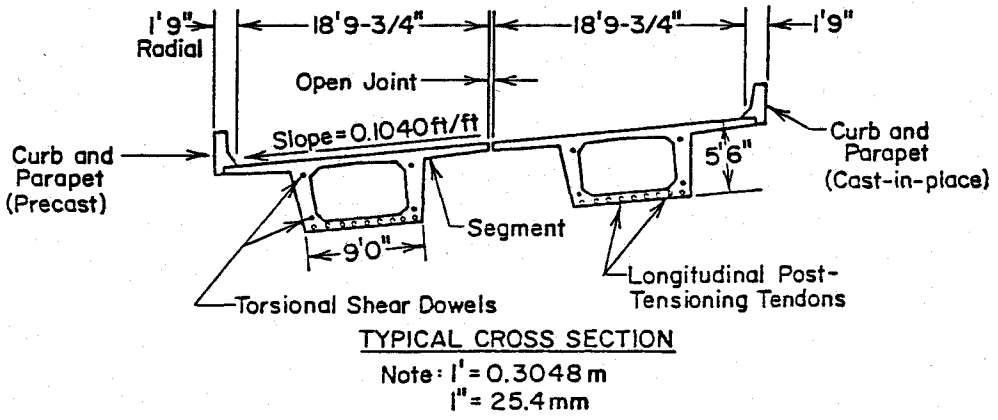


Fig. 5b. Typical cross section of experimental segmental box girder bridge.

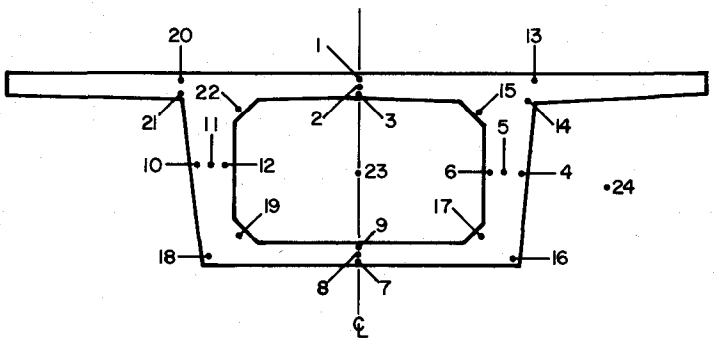


Fig. 6. Location of thermocouples in box girder transverse temperature study (Midspan Segment 9A).

## TEST BRIDGE

Field observations were recorded for a segmental prestressed box girder bridge located at the Pennsylvania Transportation Research Facility. The test bridge consisted of two curved, superelevated, prestressed box girders, each composed of 17 segments, as shown in Fig. 5. The topography of the site consisted of gentle rolling hills with a complete lack of large obstacles. Hence, maximum solar radiation was incident on the bridge surface. Also, the open terrain allowed the extremes of the thermal conditions to be observed, including wind-induced convection.

The instrumentation for measuring temperatures consisted of an Esterline Angus-Model E1124E multipoint recorder and 24 copper versus constantan thermocouples which were located on the cross section as shown in Fig. 6. The thermocouple placement was performed after bridge erection by drilling and filling the void with an epoxy which was specified by the manufacturer as thermally compatible with the concrete.

Calibration was performed by comparison of the ambient air temperature of the interior cavity, as determined by a mercury thermometer, to a freely exposed thermocouple within the cavity of the girder. Overall expected optimal precision of the temperature measurements was approximately $\pm 1.5°F$ ($\pm 0.8°$ C).

The average critical deflections at midspan were also measured using six dial gages with two placed at each end and two placed at midspan. The appropriate weather information was obtained from the Meteorology Observatory at The Pennsylvania State University, located approximately 5 miles (8 km) southeast of the test site. The second source of meteorological information was the University Park Airport, located approximately 1 mile (1.6 km) south of the bridge location.

## FIELD STUDY

The initial portion of the thermal study considered the possibility of a longitudinal temperature variation. This investigation compared ten thermocouple readings at hourly intervals for three different diurnal (daily) cycles between Segments 2A and 5A, and 2A and 9A (see Fig. 5). The field readings consisted of readings at Segments 2A and 5A on June 30, 1978, and at Segment 2A and Segment 9A on July 11, 1978, and August 22, 1978, for ten thermocouple locations in each cross section.

The collected ordered pairs of readings for like thermocuple positions were then analyzed by simple linear regression. From the regression analysis, it was concluded that there was no significant longitudinal temperature variation. Therefore, since the temperature distribution was found to be constant in the longitudinal direction, it was concluded that curvature due to temperature was also constant along the length of the beam. The longitudinal study reduced the heat flow problem from a three-dimensional analysis to one with no more complexity than two dimensions.

The second portion of the study observed the midspan vertical deflections and transverse temperature distributions of the bridge for 18 diurnal (daily) cycles during the period starting on October 25, 1978, and ending on October 16, 1979. The set of 18 diurnal observations was designed to indicate seasonal extremes as best as could be predicted by the researchers prior to the measurements.

Each transverse temperature distribution was compiled from the 24 thermocouple readings, and the corresponding midspan vertical deflections were determined for every hour starting at midnight and ending at midnight, 24 hours later. The deflection readings were then referenced to the equilib-

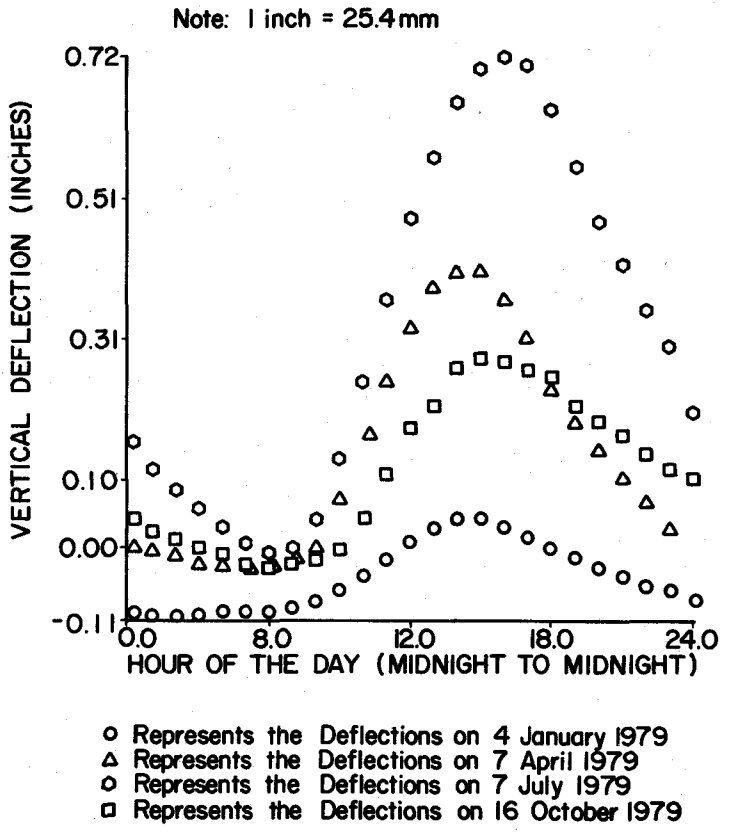


Fig. 7. Vertical deflections (uniform temperature distribution used as reference).

rium position of the experimental box girder bridge under prestressed loading, dead loading, and a uniform temperature distribution.

## OBSERVATIONS AND FINDINGS

The effect of the seasonal variation is shown in Fig. 7. The observations showed that the maximum upward deflection, 0.72 in. (18.29 mm), occurred on July 7, 1979, and the maximum downward deflection, 0.11 in. (2.79 mm), occurred on January 4, 1979. The thermal conditions on July 7, 1979, included a maximum air temperature of 86°F (30.0°C), a minimum temperature of 64°F (17.8°C), a 24-hour wind movement of 60 miles (97 km) with no prevailing direction, a clear to hazy sky condition, and a cumulative solar radiation of 660.2 Langleys. The 3 days prior to July 7, 1979, had similar weather conditions.

On January 4, 1979, the weather was completely the opposite, with a temperature range of +12 to −2°F (−11.1 to −25.1°C), a 24-hour wind movement of 208 miles (1098 km) from the west, the presence of snow flurries, and a cumulative solar radiation of 122.9 Langleys. For several days prior to January 4, the weather was consider-

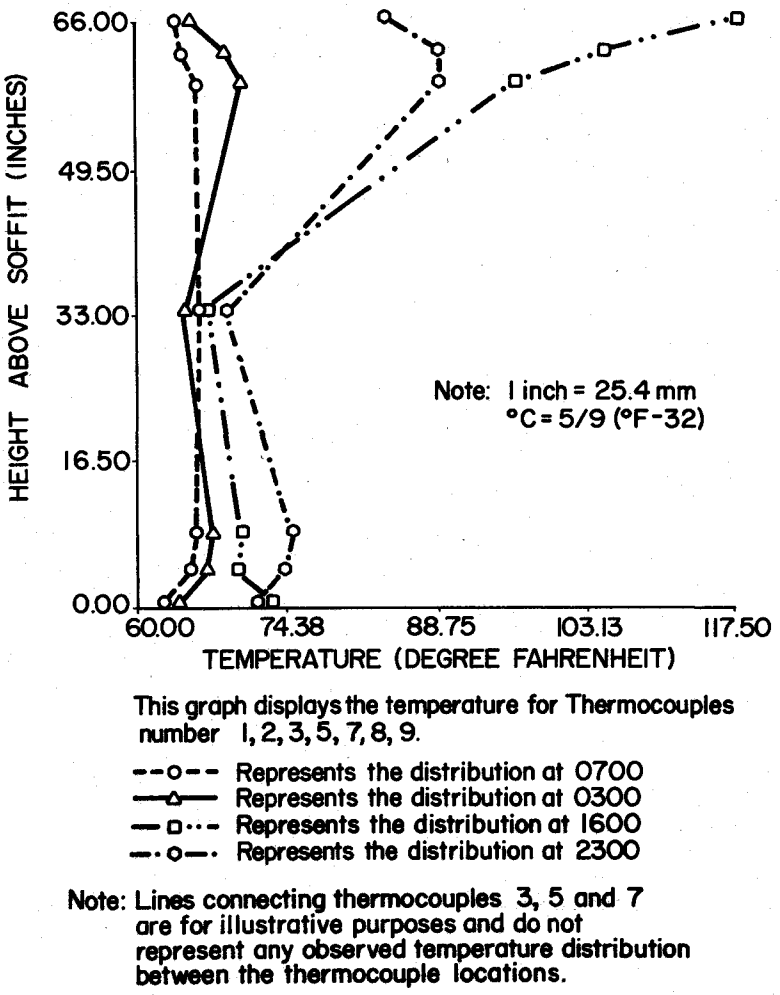


Fig. 8. Vertical temperature distribution on July 7, 1979.

ably warmer with wider air temperature ranging from +38 to −2°F (3.3. to −18.9°C).

The thermocouple readings (Locations 1, 2, 3, 5, 9, 8, and 7) for various hours on July 7, 1979, are shown in Fig. 8. The maximum upward deflection, 0.72 in. (18.3 mm), occurred at 4:00 p.m., resulting in a maximum surface temperature differential equalling 51°F (28.3°C) (difference between readings for Thermocouples 1 and 5).

Note that throughout the study, temperature differentials were taken relative to Thermocouple 5 since this location showed very little temperature fluctuation during the diurnal cycle. The relatively small temperature range of Thermocouple Location 5 (shown in Fig. 8) was characteristic of every diurnal set of observations; hence, Thermocouple Location 5 was taken as the seasonal temperature of the cross section.

A comparison of the 4:00 p.m. temperature distribution on July 7, 1979

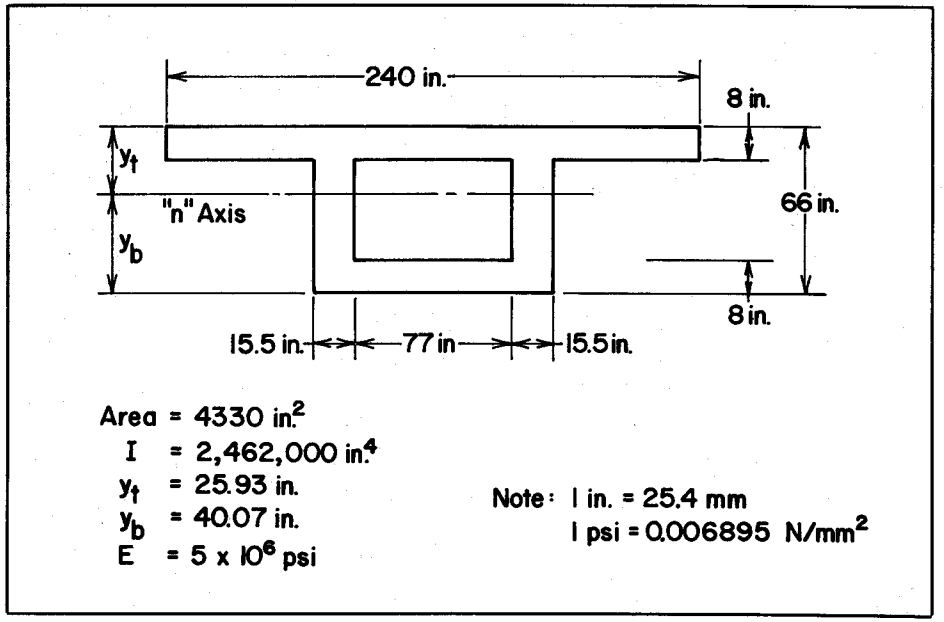


Fig. 9. Simplified cross section of box girder.

(see Fig. 8) with the New Zealand Specification [see Fig. 4(a)] shows rather good agreement. The observed maximum surface temperature differential, 51°F (28.3°C), is reasonably close to the New Zealand recommendation of 32°C (57.6°F).

This agreement is further reinforced by the fact that Thermocouple Location 5 did indicate some small increasing temperature during the day. If these increasing temperatures were accounted for in the temperature distributions, a somewhat higher value of surface temperature differential would result.

Another strong agreement between the observations and the New Zealand Specification is that at the maximum upward deflection, the temperature in Thermocouple Locations 1, 2, and 3 indicates a pattern which is in close agreement with the linear distribution specified by the New Zealand Code.

In summary, the field observations appear to indicate that the critical temperature distribution that causes maximum upward bowing can be approximated by a fifth-order polynomial. In addition, the slab above the box cell showed a linear temperature distribution. The question of accuracy versus complexity, however, still remains.

In order to answer this question, the observed curvature, which was calculated from measured vertical deflections, was compared with theoretical curvatures which were calculated from both the modified New Zealand Specifications and the modified PCI-PTI temperature distribution method.

## NUMERICAL COMPARISONS

The temperature distributions given in Fig. 4 were modified to conform with field observations. The resulting curvatures were determined from Eq. (2) and the resulting average strains were determined from Eq. (3) using the generalized cross section shown in Fig. 9. The corresponding stresses were also determined using Eq. (1).

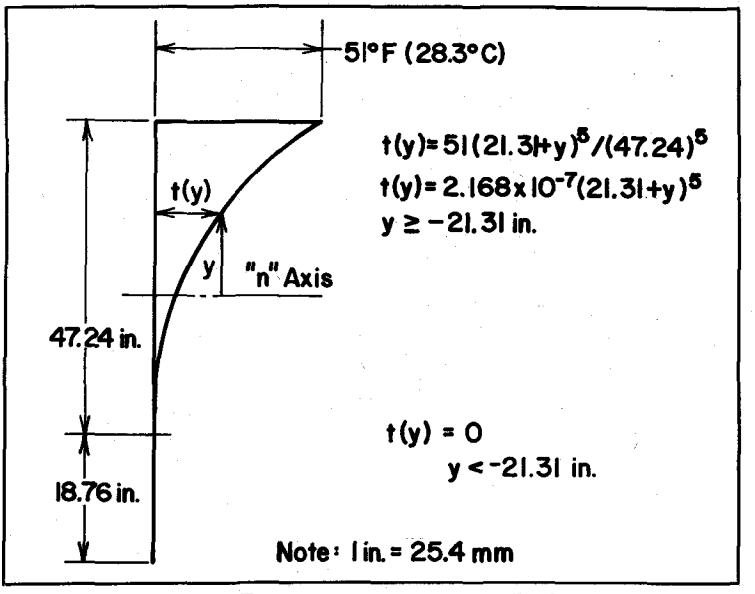

Fig. 10. Modified New Zealand temperature distribution.

## EXAMPLE 1

A fifth-power temperature distribution was assumed across the entire cross section, including the deck above the box section, with the triangular temperature distribution at the bottom neglected. This distribution is shown in Fig. 10, and it is used in determining the curvature and strain.

### A. Curvature

$$\phi = \frac{\alpha}{I}\int_{-y_b}^{+y_t} t(y)\cdot b(y)\cdot y\cdot dy \qquad (2)$$

$$= \frac{\alpha}{I}\left[\int_{-40.07}^{-21.31} (0°\text{F})\cdot b(y)\cdot y\cdot dy + \int_{-21.31}^{+17.93} (2.168\times 10^{-7})(21.31+y)^5(2)(15.5)(y)\,dy + \int_{+17.93}^{+25.93} (2.168\times 10^{-7})(21.31+y)^5(240)(y)\,dy\right]$$

$$= \frac{\alpha}{I}\left[(6.72\times 10^{-6})[(1/7)(21.31+y)^7 - (21.31/6)(21.31+y)^6]_{-21.31}^{+17.93} + (5.20\times 10^{-5})[(1/7)(21.31+y)^7 - (21.31/6)(21.31+y)^6]_{+17.93}^{+25.93}\right]$$

$$= (\alpha/I)[1{,}508{,}000]$$

$$= (6\times 10^{-6}/2{,}462{,}000)[1{,}508{,}000]$$

$$\phi = 3.68\times 10^{-6}\ 1/\text{in.}\ (0.145\times 10^{-6}\ 1/\text{mm})$$

### B. Elongation Strain Due to Mean Temperature Distribution

$$\epsilon_{ave} = \frac{\alpha}{A}\int_{-y_b}^{+y_t} t(y) \cdot b(y) \cdot dy \qquad (3)$$

$$= \frac{\alpha}{A}\left[\int_{-40.07}^{-21.31} (0°F) \cdot b(y) \cdot dy + \int_{-21.31}^{+17.93} (2.168 \times 10^{-7}) \times (21.31 + y)^5 (2)(15.5)\, dy + \int_{+17.93}^{+25.93} (2.168 \times 10^{-7})(21.31 + y)^5 (240)\, dy\right]$$

$$= \frac{\alpha}{A}\left[6.72 \times 10^{-6} \ (1/6)(21.31 + y)^6 \Big|_{-21.31}^{+17.93} + (5.20 \times 10^{-5})(1/6)(21.31 + y)^6 \Big|_{+17.93}^{+25.93}\right]$$

$$= (\alpha/A)(68{,}770)$$

$$= (6 \times 10^{-6}/4330)[68{,}770]$$

$$\epsilon_{ave} = 9.53 \times 10^{-5} \text{ in./in.}$$

### C. Stress Development

$$f(y) = E[\phi \cdot y + \epsilon_{ave} - \alpha \cdot t(y)] \qquad (1)$$

$$= 5 \times 10^6 [3.68 \times 10^{-6} \cdot y + 9.53 \times 10^{-5} - (6 \times 10^{-6}) \times (2.168 \times 10^{-7})(21.31 + y)^5]$$

$$f(y) = 18.4y + 476.5 - 6.50 \times 10^{-6}(21.31 + y)^5$$

The stresses predicted from the fifth power temperature distribution are shown in Fig. 11.

## EXAMPLE 2

A uniform temperature distribution of 35.8°F (19.9°C) in the flange gives the same average cross-sectional temperature (same $\epsilon_{ave}$) as the fifth-power temperature distribution used in Example 1, and is shown in Fig. 12. This uniform temperature is used below:

### A. Curvature

$$\phi = (6 \times 10^{-6}/2{,}462{,}000)[35.8 \cdot 240 \cdot 21.93 \cdot 8] \qquad (2)$$

$$= 3.67 \times 10^{-6} \text{ 1/in. } (0.144 \times 10^{-6} \text{ 1/mm})$$

### B. Effect of Mean Temperature Distribution

$$\epsilon_{ave} = (6 \times 10^{-6}/4330)[35.8 \cdot 240 \cdot 8]$$

$$= 9.53 \times 10^{-5} \text{ in./in.} \qquad (3)$$

### C. Stress Development

$$f(y) = 5 \times 10^6 [3.67 \times 10^{-6} \cdot y + 9.53 \times 10^{-5} - 6 \times 10^{-6} \cdot t(y)] \qquad (1)$$

$$= 18.35y + 476.5 - 30 \cdot t(y)$$

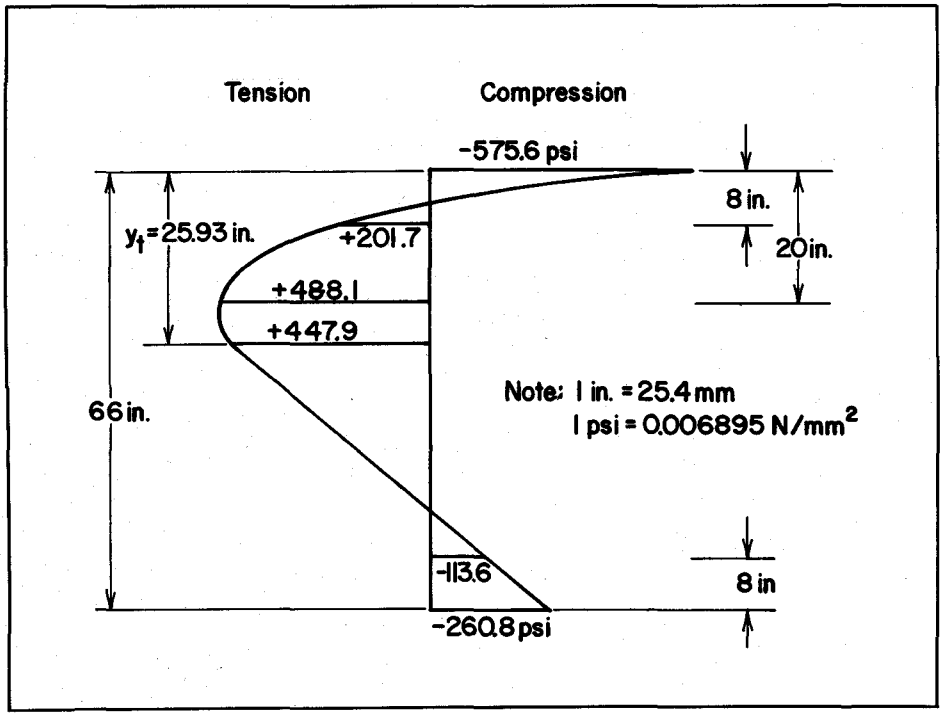


Fig. 11. Stresses predicted from modified New Zealand temperature distribution.

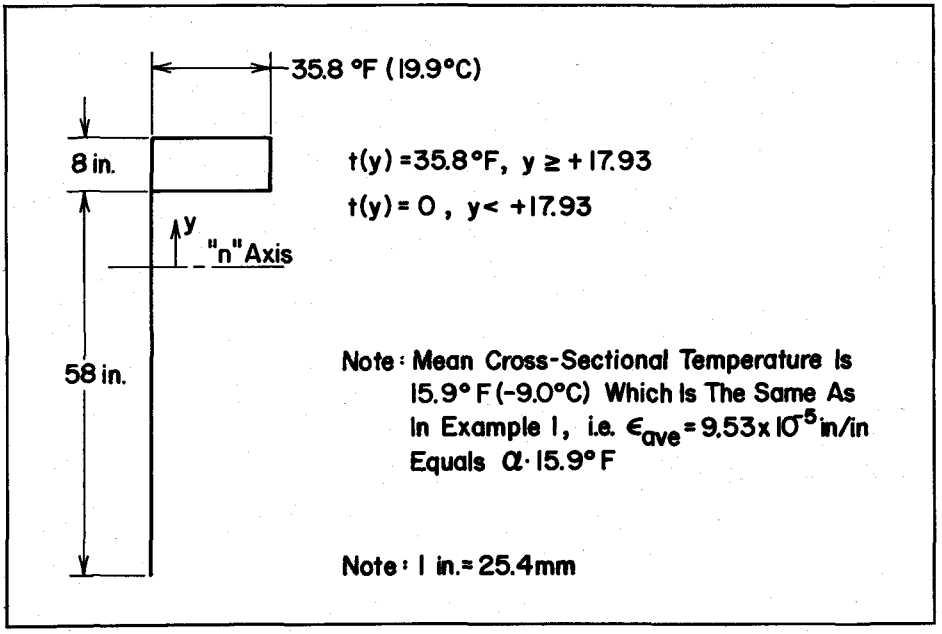


Fig. 12. Modified PCI-PTI temperature distribution.

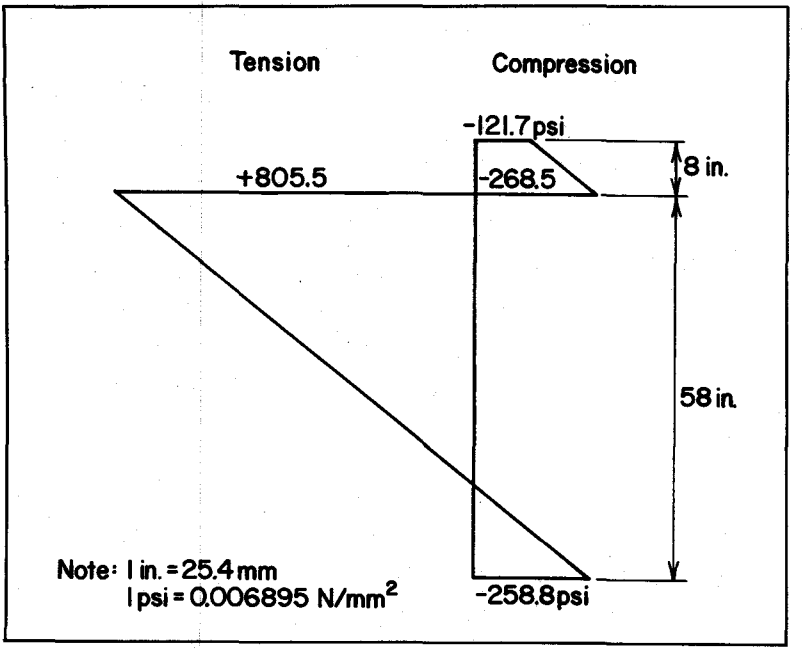


Fig. 13. Stresses predicted from modified PCI-PTI temperature distribution.

The stresses predicted from the uniform temperature distribution in the flange are shown in Fig. 13.

From Examples 1 and 2, it is evident that the basic assumptions lead to approximately the same curvature but markedly different stress patterns.

## COMPARISON OF OBSERVED VALUES

The observed critical curvature was determined from the vertical deflection measurements. With the presence of 51°F (28.3°C) temperature difference between flange surface and the temperature at Thermocouple 5, the test bridge bowed upward 0.72 in. (18.29 mm) from the dead load prestressed equilibrium position. In addition, since it was concluded that temperature was constant longitudinally, then curvature must be constant also.

Therefore, with the application of both the first and second moment-area principles, the midspan deflection multiplied by $8/L^2$ results in curvature, where $L$ is taken as the beam length. Hence, for a midspan deflection equalling 0.72 in. (18.3 mm) and a beam length equalling 118.08 ft (35.99 m), an experimental curvature equalling 2.87 x $10^{-6}$ 1/in. (0.113 x $10^{-6}$ 1/mm) was computed.

The experimental curvature computed above was based upon the assumption that the upward deflection of 0.72 in. (18.3 mm) was associated with an ideal simply-supported beam. However, there was evidence that there were some end restraints that inhibited the structure from functioning in the ideal fashion. If these restraints had not been present, the upward deflection would have been greater, and the experimental curvature would have been correspondingly greater.

In fact, load tests on the experimental bridge[8] indicated that the experimental

curvature for standard truck load was 22 percent less than the theoretical curvature as determined from moment-area principles. If a similar discrepancy is accounted for in the present case, the experimental curvature would be 3.68 x $10^{-6}$ 1/in. (0.145 x $10^{-6}$ 1/mm), which agrees closely with the computed value of 3.67 x $10^{-6}$ 1/in. (0.144 x $10^{-6}$ 1/mm).

Therefore, from an overall comparison, the field observations seemed to substantiate curvature predictions from the computation using a fifth-order temperature distribution or a uniform flange temperature distribution. However, for the uniform flange temperature, a flange temperature equalling about twice the currently proposed PCI-PTI value had to be used.

A commonly used method for computing curvature is to assume a linear temperature distribution from the middle of the top slab to the middle of the bottom slab. It should be pointed out, however, that this temperature distribution produces no thermal stresses in a statically determinate structure. It was determined by calculations that a 35.6°F (19.8°C) temperature difference between the top and bottom slab with a linear variation in between produces the same theoretical curvature, 3.67 x $10^{-6}$ 1/in. (0.0145 x $10^{-6}$ 1/mm), as the temperature distribution in Examples 1 and 2.

## CONCLUSIONS FOR DESIGN

There was no significant longitudinal temperature variation in the experimental segmental bridge. Therefore, curvature due to temperature was constant along the length of the girder, and the heat flow problem was reduced from a three-dimensional to a two-dimensional state. Further, it was found that there was very little transverse temperature variation in the horizontal direction.

The maximum transverse temperature differential in the vertical direction was measured as 51°F (28.3°C) and occurred at the same time as the maximum upward deflection. This showed a rather good agreement with the New Zealand Specification which recommends 57.6°F (32°C). The field observations also indicated that the critical temperature distribution can be approximated by a fifth-order polynomial in the webs, and that a linear temperature distribution exists in the slab above the box section, as recommended in the New Zealand Specification.

Either a fifth-order temperature distribution across the entire cross section (New Zealand gradient) or a uniform temperature distribution in the top slab (PCI-PTI gradient) produces a curvature which agrees with experimental values; however, temperature stresses produced by the two temperature distributions differ markedly. The uniform temperature distribution in the slab of 35.8°F (19.9°C) which agrees with experimental curvatures is approximately twice the PCI-PTI recommended value of 18°F (10°C).

The consideration of curvature due to temperature is important in design, especially in indeterminate structures where temperature stresses due to continuity will superimpose on the temperature stresses due to the temperature distribution. If the temperature stresses due to the temperature distribution and/or continuity induced stresses exceed the ultimate tensile stress of the concrete, reinforcing steel must be provided to carry the total tensile load.

## ACKNOWLEDGMENTS

This study covers only a portion of a major 6-year investigation on an experimental segmental bridge which was conducted at The Pennsylvania Transportation Institute located at The Pennsylvania State University, University Park.

The study was sponsored and funded by the Pennsylvania Department of Transportation and the Federal Highway Administration.

The contents of this paper reflect the views of the authors who are responsible for the facts and the accuracy of the data. The contents do not necessarily reflect the official views or policies of the sponsors.

## REFERENCES

1. Priestley, M. J. N., "Thermal Gradients in Bridges: Some Design Considerations," *New Zealand Engineering*, V. 27, No. 7, July 1972, pp. 228-233.
2. Price, W. J., "Introductory Note," *Bridge Temperatures*, TRRL Report SR 442, Transport and Road Research Laboratory, Crowthorne, England, 1978.
3. Priestley, M. J. N., "Design of Concrete Bridges for Temperature Gradients," *ACI Journal*, V. 75, No. 5, May 1978, pp. 209-217.
4. Priestley, M. J. N., and Buckle, I. G., "Ambient Thermal Response of Concrete Bridges," RRU Bulletin 42, Roads Research Unit, National Road Board, Wellington, New Zealand, 1979.
5. AASHTO, *Standard Specifications for Highway Bridges*, American Association of State Highway and Transportation Officials, 12th edition, Washington, D.C., 1977.
6. *Precast Segmental Box Girder Bridge Manual*, Published jointly by the Prestressed Concrete Institute (Chicago, Illinois) and Post-Tensioning Institute (Phoenix, Arizona), 1978, pp. 41-44.
7. Hoffman, P. C., McClure, R. M., and West, H. H., "Temperature Studies for an Experimental Segmental Bridge," Interim Report, Research Project No. 75-3, Report PTI 8010, Pennsylvania Transportation Institute, The Pennsylvania State University, University Park, Pennsylvania, June 1980.
8. McClure, R. M., and West, H. H., "Field Testing of an Experimental Segmental Bridge," Interim Report, Research Project No. 75-3, Report PTI 8009, Pennsylvania Transportation Institute, The Pennsylvania State University, University Park, Pennsylvania, June 1980.

## APPENDIX

For the purposes of illustration, consider an externally statically determinate truss structure and a temperature differential, as shown in Fig. A1 (a). Since the truss is internally statically determinate, heating the top and middle members by $4\Delta T$ and $\Delta T$ causes them to elongate $4\alpha\Delta TL$ and $\alpha\Delta TL$, respectively, where $\alpha$ is the coefficient of thermal expansion and $L$ is the member length. This in turn causes the truss members to rotate in order to accommodate the increases in member lengths. Note that this reconfiguration only changes the interior triangular configuration without introducing stress.

In contrast, if the truss is made internally statically indeterminate and is subjected to the same member temperature differential, a stress-free condition does not exist [see Fig. A1 (b)]. Since there are internal redundancies, a geometrical reconfiguration causes some truss members to contract and others to elongate beyond that required by member temperature equilibrium; hence, stresses are developed.

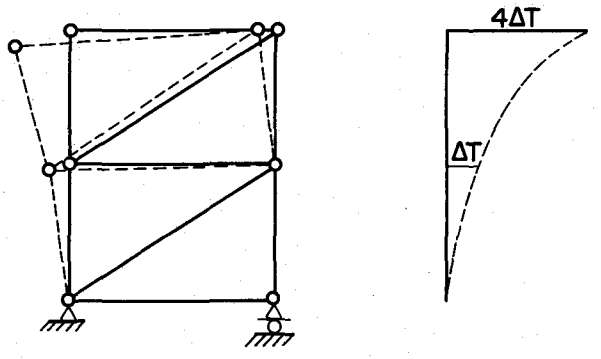


(a) Internally Statically Determinate Truss and Chord Temperature Differential

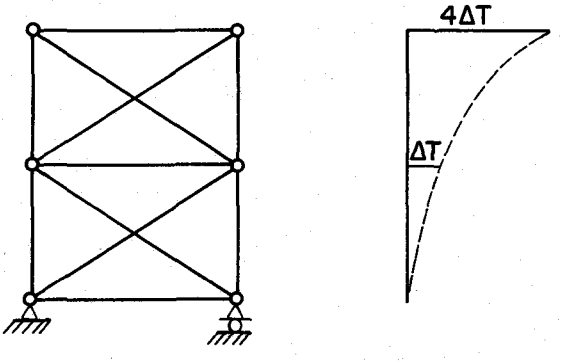


(b) Internally Statically Indeterminate Truss and Chord Temperature Differential

Fig. A1. Determinate and indeterminate trusses and chord temperature differentials.

For example, because of the diagonal redundancies, the top member expands a length, $\Delta L$, which is smaller than $4\alpha\Delta TL$. This results in a compressive strain:

$$\epsilon_c = \frac{\Delta L}{L} - 4\alpha\Delta T$$

which causes a compressive stress:

$$f_c = E\left(\frac{\Delta L}{L} - 4\alpha\Delta T\right)$$

where $E$ equals the modulus of elasticity.

This residual stress concept can be generalized for an externally statically determinate beam and a nonuniform temperature differential, as shown in Fig. A2. In this case, the beam can be viewed as an internally indeterminate truss to an infinite degree. The only possible physical response of the beam to a temperature differential is a bowing upwards or sagging downward, giving a linear strain distribution ac-

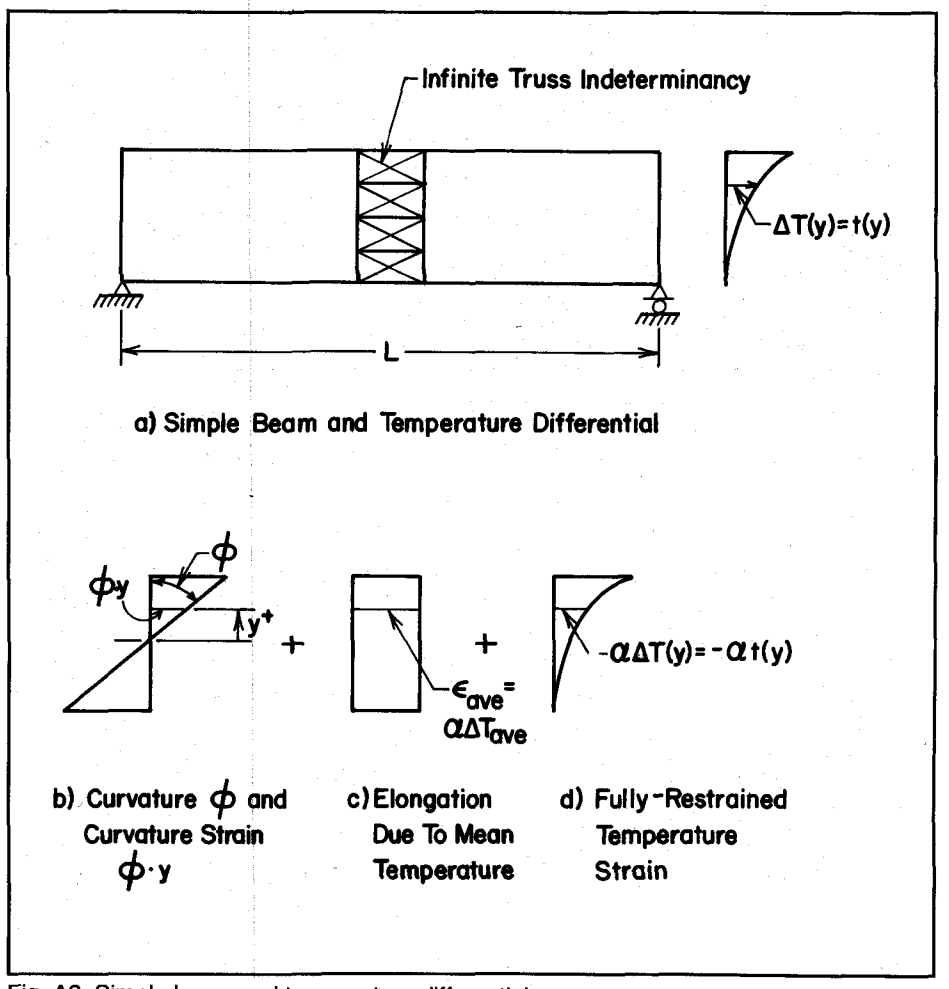


Fig. A2. Simple beam and temperature differential.

cording to the Bernoulli-Navier principle [see Fig. A2 (b)].

In addition, elongation or contraction strain develops due to the mean temperature effect [see Fig. A2 (c)]. Each longitudinal fiber, however, has a temperature strain requirement of $\alpha\Delta T(y)$ associated with full restraint, as shown in Fig. A2 (d). Hence, as in the simple truss example, a residual stress problem exists, as follows:

$$f_r(y) = E[\phi y + \epsilon_{ave} - \alpha t(y)]$$

where

$t(y)$ = temperature change, $\Delta T$, at a distance $y$ from the neutral axis

**NOTE:** Discussion of this paper is invited. Please submit your discussion to PCI Headquarters by Nov. 1, 1983.